Influence of nonlinear loss competition on pulse compression and nonlinear optics in silicon

En-Kuang Tien, Feng Qian, Nuh S. Yuksek, and Ozdal Boyraz

Citation: Applied Physics Letters **91**, 201115 (2007); doi: 10.1063/1.2807273
View online: http://dx.doi.org/10.1063/1.2807273
View Table of Contents: http://scitation.aip.org/content/aip/journal/apl/91/20?ver=pdfcov
Published by the AIP Publishing

Influence of nonlinear loss competition on pulse compression and nonlinear optics in silicon

En-Kuang Tien,[a] Feng Qian, Nuh S. Yuksek, and Ozdal Boyraz
EECS Department, University of California, Irvine, California 92697, USA

(Received 8 August 2007; accepted 19 October 2007; published online 16 November 2007)

Aggregate nonlinear response of silicon is determined by the competition between the free carrier absorption (FCA) and two-photon absorption (TPA). We show that the front end of optical pulses is always exposed to TPA dominated nonlinear regime, whereas the trailing edge can be seen at FCA dominated regime at high intensities. These two losses can be used for pulse compression if the center of the pulse is in FCA dominated nonlinear regime. To reach this operation regime, energy of 50 ps wide pulses has to be larger than 50 nJ (40 GW/cm^2). Competition phenomenon is observed experimentally in a mode locked laser setup to generate 60 ps pulse of 60 nJ. © *2007 American Institute of Physics*. [DOI: 10.1063/1.2807273]

Nonlinear optics appears to be the enabling technology for complementry metal-oxide semiconductor compatible active photonic devices in silicon. In particular, the Raman effect[1,2] and two-photon absorption[3,4] (TPA) have been investigated extensively to provide low cost solutions to photonic industry. Recently, chip scale Raman lasers pumped by commercial diode lasers[5] and fast electro-optic modulators operating up to 30 Gbits/s have been demonstrated.[6,7] Similarly, Kerr nonlinearity and TPA have been utilized for ultrafast applications such as parametric wavelength converters,[8,9] supercontinuum generators,[10,11] and autocorrelators.[12] Although most of the nonlinear devices are designed for steady state response, in ultrafast applications, the transient behaviors of TPA and TPA induced free carrier concentration have prominent effect on the final outcome.[9,10,13–15] In particular, pulse shaping and pulse chirping due to free carrier plasma effect are predominantly determined by the competition between TPA and TPA induced free carriers in nonlinear devices.

Recently, we proposed and demonstrated an approach for pulse compression and laser modelocking using free carrier transient effects.[13] Here, we present theoretical and experimental studies of free carrier absorption (FCA) transients and TPA with special emphasis on their effects on self-pulse compression. To assess this competition and its effects on the pulse compression, we calculate the temporal behavior of TPA and FCA generated by 10–1000 ps wide optical pulses with peak intensities up to 40 GW/cm^2. We show that the TPA produced at the peak intensity by pulses shorter than 50 ps surpasses the free carrier losses at the trailing edge and, hence, produces net pulse broadening even at 50 nJ pulse energy values (40 GW/cm^2 peak intensity). As the pulse energy increases to 500 nJ by increasing the pulse width, the losses at the trailing edge dominate and produce 40% pulse compression ($\tau_{out}/\tau_{in} \sim 0.6$). We observe this competition in a mode locked laser setup.[13] We demonstrate that mode locking by silicon can produce 60 ps optical pulses with 60 nJ pulse energy inside the laser cavity. Without the aid of self-phase modulation and dispersive pulse shaping, the shortest pulse to be generated will be limited by the TPA dominated pulse broadening.

The pulse envelope evolution in the presence of optical nonlinearities is conventionally estimated by solving the nonlinear Schrödinger equation,[10,16]

$$\frac{\partial E(t,z)}{\partial z} = -\frac{1}{2}[\alpha + \alpha_{FCA}(t,z) + \alpha_{TPA}(t,z)]E(t,z) - i\gamma|E(t,z)|^2E(t,z) + i\frac{2\pi}{\lambda}\Delta n(t,z)E(t,z), \quad (1)$$

where E, α, γ, and Δn represent the electric field, attenuation constants, the effective nonlinearity, and the free carrier induced index change, respectively. The pulse shaping is determined by the nonlinear losses on the right hand side of Eq. (1). Among two nonlinear loss terms, the TPA,

$$\alpha_{TPA} = \frac{1}{z}\ln(1 + \beta I_0 z), \quad (2)$$

is an intensity dependent and memoryless attenuation following the pulse shape. Here, β is the TPA coefficient [0.45 cm/GW at 1550 nm (Ref. 12)], A_{eff} is the effective area of the waveguide, and I_0 is the intensity. However, the FCA,

$$\alpha_{FCA}(z,t) = 1.45 \times 10^{-17}\left(\frac{\lambda}{1.55}\right)^2 N(z,t)\ (\mathrm{cm}^{-1}), \quad (3)$$

has memory and is accumulative.[13] For cw signals or signals wider than free carrier recombination time τ_0, free carrier densities will be stabilized at a local $N(z)$ value of $N(z) = \tau_0\beta I^2(z)/2h\nu$ after $\sim\tau_0$. On the other hand, time varying optical signals with pulse width smaller than τ_0 will result to different time dependent local free carrier densities and FCA along the waveguide governed by the equation,

$$\frac{dN(t,z)}{dt} = -\frac{N(t,z)}{\tau_0} + \beta\frac{I^2(t,z)}{2h\nu}. \quad (4)$$

To estimate pulse shaping, time and space dependent free carrier density, $N(z,t)$, and the nonlinear losses are the utmost important parameters to be determined. Based on the peak intensity and the pulse energy, the nonlinear response of silicon can be divided into two separate regimes in time and in space: the TPA dominated regime and the FCA dominated regime.[9] Figure 1 illustrates the calculated outcome of two different regimes for 20 and 500 ps optical pulses with 1 kW peak power (i.e., 20 and 500 nJ pulse energies). The waveguide is 1 cm long with 5 μm^2 effective area and 16 ns free carrier lifetime. The fixed 1 kW peak power facilitates the

[a]Electronic mail: etien@uci.edu

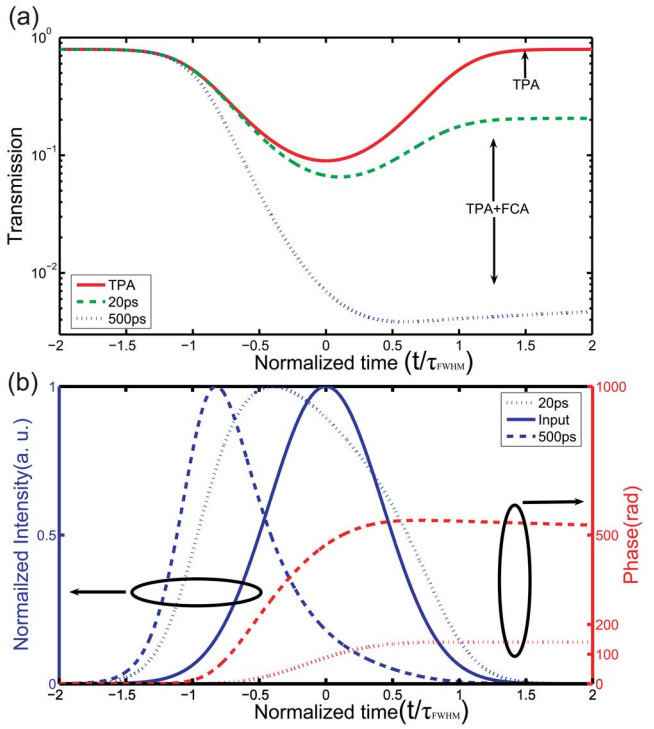

FIG. 1. (Color online) (a) TPA and free carrier loss profiles of 20 ps and 500 ps wide input pulses. (b) Estimated output pulses and chirp induced by free carrier plasma effect. The front end of both pulses are under TPA dominant nonlinear regime. However, due to excess free carriers, the trailing edge of 500 ps pulse is under FCA dominant nonlinear regime. The time axis is normalized with input pulse width for comparison purposes.

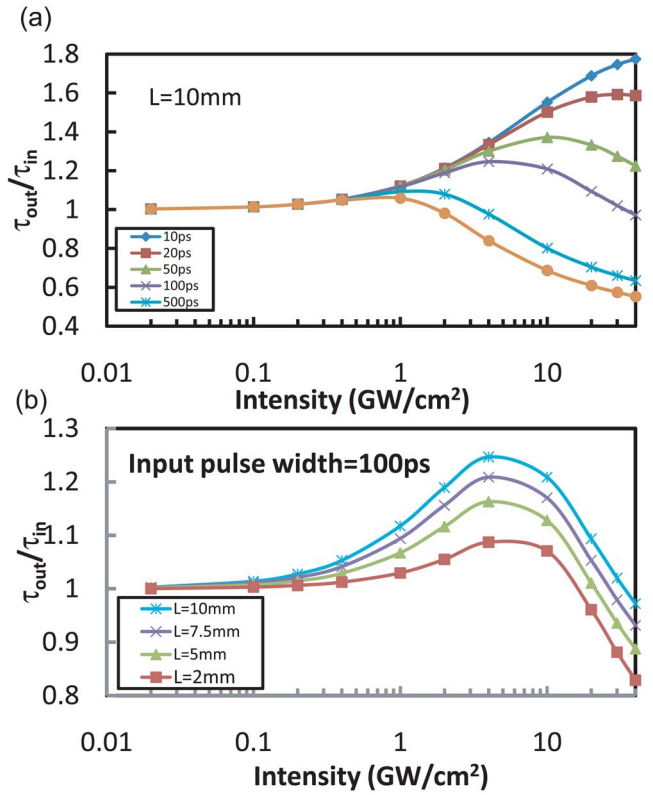

FIG. 2. (Color online) Predicted pulse compression ratio in (a) 10 mm long silicon waveguide for different initial pulse widths and (b) silicon waveguides with different lengths.

same level of TPA (90%) at the center for comparison [Fig. 1(a)]. However, FCA generated by 500 nJ pulse is 40 times stronger than the FCA generated by 20 ps pulses at the same peak intensity due to difference in number of absrobed photons. We estimate that while 20 nJ pulses are being broadened due to the TPA dominance, 500 nJ pulses are being compressed to 350 ps by FCA dominance [Fig. 1(b)]. Here, results are presented in normalized time unit t/τ_{FWHM}, where τ_{FWHM} is the pulse width at the input, to have better comparisons of output pulses for different input conditions and to have a better visualization. The free carrier plasma effect is always present and, unlike FCA and TPA competitions, produces a steady linear phase change across the pulse. However, due to the larger free carrier density, high energy pulses experience approximately four times larger phase change across the pulse [Fig. 1(b)]. A blueshifted spectral broadening has been attributed to this phase change when it is combined with self-phase modulation, as reported previously.[10]

The losses presented here represent aggregate attenuation at the end of the waveguide. We expect that the total waveguide length, the input pulse width, and the pulse energy will have prominent influence on the final outcome. Figure 2(a) illustrates the compression behavior of 10–1000 ps optical pulses in a 1 cm long silicon waveguide. At low peak powers, $<10^{16}$ cm^{-3} carriers are generated to facilitate attenuation of the trailing edge and to provide self-compression.[13] However, stronger TPA at the center of the pulse dominates at these intensities and induces net pulse broadening at 3 dB point. Free carrier dominance is expected at higher intensities. For example, 1 ns pulses with 2 GW/cm^2 intensities generate 4×10^{18} cm^{-3} free carriers which dominate over TPA at the center of the pulse and facilitate net self-compression. For 500 and 100 ps wide optical pulses, it requires 3 GW/cm^2 (75 nJ) and 32 GW/cm^2 (160 nJ), respectively, to initiate the same type of compression. For input pulses shorter than 50 ps, the TPA induced pulse broadening surpasses the self-compression even at 40 GW/cm^2 and, hence, net pulse broadening is expected. However, we should note that, simple free carrier density calculations may not be reliable at such a high intensity due to Auger recombination.[17] For instance, as the free carrier density increases from 10^{18} to 10^{19} cm^{-3}, the free carrier lifetime due to Auger effect will reduce from $\sim$1.3 to $\sim$20 ns, which is comparable to the free carrier lifetime of our waveguides.

Figure 2(b) demonstrates the effect of waveguide length on the pulse compression. For longer waveguides, the front end facilitates FCA dominated behavior with $>10^{18}$ cm^{-3} free carriers. On the other hand, the back end operates in TPA dominated regime and contributes on pulse broadening and loss. Specifically, the free carrier density at the trailing edge of 100 ps pulse is estimated to be $\sim10^{19}$ cm^{-3} at the input facet. The same density drops to 10^{18} and to 2×10^{17} cm^{-3} at $L=2$ mm and at $L=10$ mm, respectively. As a result, the largest compression occurs within the first $\sim$2 mm due to FCA dominance, and then TPA induced pulse broadening dominates in the following $\sim$8 mm waveguide segment. Hence, for 100 ps input pulses, the waveguides as short as 2 mm can provide more effective pulse compression with only 50% of the peak power values used in 1 cm. These results indicate that effective utilization of TPA and FCA requires optimization of the waveguide geometry for desired pulse parameters.

The modelocking method demonstrated earlier also relies on the self-compression of optical pulses in silicon.[13] In

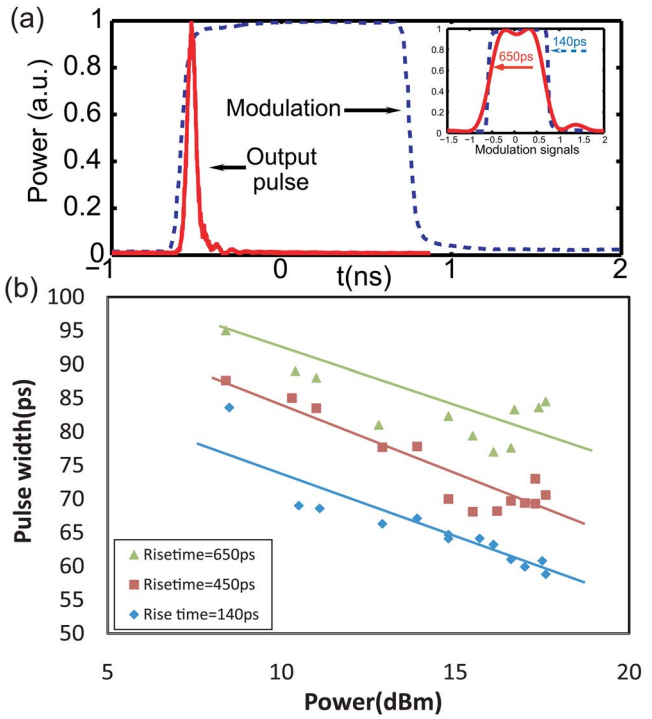

FIG. 3. (Color online) (a) Laser output for 1.5 ns pulses with 140 ps rise time. (Inset) Modulation signals used for modelocking experiment. (b) Variation of output pulse width with respect to pulse energy.

this approach, time varying losses are created via electro-optic modulation driven by >1 ns rf pulses. The final pulse width is a result of self-compression after multiple passes through the waveguide and the reamplification.[13] In order to get a short pulse at the output, the power levels and modulation signal should be set to provide $\tau_{out}/\tau_{in}<1$. Experimentally, due to self-compression effect in the silicon waveguide inside the laser cavity, ~60 ps optical pulses are generated at the steady state. Since, the final pulse width is ultimately determined by the compressibility of the pulses in the laser cavity and it is an excellent manifestation of the interaction between the TPA and the FCA in a laser setup.

Experimentally, we study how peak power and pulse energy affect the final pulse width. We use the same laser configuration[13] formed by an erbium doped fiber amplifier gain medium and a 1.7 cm long silicon waveguide pulse compressor with ~5 μm^2 effective area. The total fiber-to-fiber loss of the waveguide is measured to be ~2 dB. The output of the waveguide is connected to a 3/97 tap coupler where 3% is used as an output and 97% is fed into the electro-optic (EO) modulator. To initiate pulse formation and pulse compression by transient effects, 1.5 ns wide rectangular rf pulses with 1 MHz repetition rate are applied to an EO modulator. A 10 GHz photodetector and a 20 GHz sampling oscilloscope are used as diagnostics.[13] Since the pulse compression is intensity square dependent, at constant pulse width, the variation of rise and fall times can be used to tune the pulse energy and, hence, the number of free carriers generated by an optical pulse at fixed peak power. We use low pass rf filters with cutoff frequencies of 800 and 500 MHz to tune rise and fall times of 1.5 ns electrical signals from 140 (without filter) to 450 and 650 ps, respectively (Fig. 3).

Figure 3(a) illustrates the pulse widths measured at the laser output for different peak powers and different rise/fall times. The shortest pulse width is measured to be 60 ps by using rf signals with 140 ps rise/fall time (Fig. 3(a) inset). Figure 3(b) shows the tendency of the pulse compression with respect to different peak powers and different rise/fall times. At fixed pulse energy, slower rise time results in a fewer free carrier generations. As a result, the pulse width increases to 85 ps if the rise time is tuned to 650 ps for the same pulse energy. These measurements indicate that the free carrier concentration increases more rapidly for modulation signals with sharper rise times. To compensate the slope effect, we need to increase the pulse energy to achieve the same compression [Fig. 3(b)]. This tendency agrees with the theoretical results presented in Fig. 2(a), which shows the higher power requirement for low energy pulses. For instance, to achieve 80 ps output pulses, the average power entering the silicon waveguide has to be 9, 13, and 16 dBm levels for 140, 450, and 650 ps rise and fall times, respectively. The peak power corresponding to 80 ps pulse with 9 dBm average power is ~120 W (2.4G W/cm^2). The total loss at this setting is measured to be <6 dB, of which 2 dB is the linear loss and the rest originate from the nonlinear effects.

In conclusion, the transient behavior of free carrier concentration has prominent effect on silicon based ultrafast applications. For free carrier plasma effect, this manifests itself just as a scaling of index change. However, for FCA and TPA based pulse shaping devices, aggregate responses will differ based on their operation in TPA dominant regime and FCA dominant regime. For pulse compression and modelocking, we need TPA dominant regime at the front end of the pulse and FCA dominance at the trailing edge. These two regimes come in competition. Experimental limit on 60 ps mode locked pulse generation illustrates energy dependence of this competition. Additionally, the length of the waveguide can be used to change the operation regime.

[1]O. Boyraz and B. Jalali, Opt. Express **12**, 5269 (2004).
[2]H. S. Rong, A. S. Liu, R. Jones, O. Cohen, D. Hak, R. Nicolaescu, A. Fang, and M. Paniccia, Nature **433**, 292 (2005).
[3]Y. Liu and H. K. Tsang, Appl. Phys. Lett. **90**, 211105 (2007).
[4]M. A. Foster and A. L. Gaeta, *Conference on Lasers and Electro-Optics/Quantum Electronics and Laser Science Conference and Photonic Applications Systems Technologies*, OSA Technical Digest Series (CD), (2007), Paper No. CTuY5, see (http://www.opticsinfobase.org/abstract.cfm?URI=CLEO-2007–CTuY5).
[5]H. S. Rong, S. B. Xu, Y. H. Kuo, V. Sih, O. Cohen, O. Raday, and M. Paniccia, Nat. Photonics **1**, 232 (2007).
[6]Q. F. Xu, S. Manipatruni, B. Schmidt, J. Shakya, and M. Lipson, Opt. Express **15**, 430 (2007).
[7]A. S. Liu, L. Liao, D. Rubin, H. Nguyen, B. Ciftcioglu, Y. Chetrit, N. Izhaky, and M. Paniccia, Opt. Express **15**, 660 (2007).
[8]M. A. Foster, A. C. Turner, J. E. Sharping, B. S. Schmidt, M. Lipson, and A. L. Gaeta, Nature (London) **441**, 960 (2006).
[9]R. Dekker, A. Driessen, T. Wahlbrink, C. Moormann, J. Niehusmann, and M. Forst, Opt. Express **14**, 8336 (2006).
[10]O. Boyraz, P. Koonath, V. Raghunathan, and B. Jalali, Opt. Express **12**, 4094 (2004).
[11]E. Dulkeith, Y. A. Vlasov, X. G. Chen, N. C. Panoiu, and R. M. Osgood, Opt. Express **14**, 5524 (2006).
[12]T. K. Liang, H. K. Tsang, I. E. Day, J. Drake, A. P. Knights, and M. Asghari, Appl. Phys. Lett. **81**, 1323 (2002).
[13]E. K. Tien, N. S. Yuksek, F. Qian, and O. Boyraz, Opt. Express **15**, 6500 (2007).
[14]L. Yin and G. P. Agrawal, Opt. Lett. **32**, 2031 (2007).
[15]I. W. Hsieh, X. G. Chen, J. I. Dadap, N. C. Panoiu, R. M. Osgood, S. J. Mcnab, and Y. A. Vlasov, Opt. Express **15**, 1135 (2007).
[16]X. G. Chen, N. C. Panoiu, and R. M. Osgood, Jr., IEEE J. Quantum Electron. **42**, 160 (2006).
[17]M. J. Kerr and A. Cuevas, J. Appl. Phys. **91**, 2473 (2002).